SEISMIC VELOCITY PREDICTION IN SHALLOW (< 30M) PARTIALLY-SATURATED, UNCONSOLIDATED SEDIMENTS USING EFFECTIVE MEDIUM THEORY

James M. Crane, Department of Geology & Geophysics, Louisiana State University, Baton Rouge, LA
Juan M. Lorenzo, Department of Geology & Geophysics, Louisiana State University, Baton Rouge, LA
Chris D. White, Department of Petroleum Geology, Louisiana State University, Baton Rouge, LA

Abstract

Seismic velocity models of the near-subsurface (<30 m) better explain seismic velocities when all elements of total effective stress are considered, especially in materials with large cohesive and capillary pressures such as clays. Current constitutive elastic models that predict velocities in granular materials simplify the effect of total effective stress by equating it to net overburden stress, excluding interparticle stresses. A new proposed methodology calculates elastic moduli of granular matrices in near-surface environments by incorporating an updated definition of total effective stress into Hertz-Mindlin theory and calculates the elastic moduli of granular materials by extending Biot-Gassmann theory to include pressure effects induced by water saturation changes. At shallow depths, theoretically calculated seismic velocities decrease in clay and increase in sand with an increase in water saturation because interparticle stresses suppress the Biot-Gassmann effect. For standard sand and clay properties, net overburden stress becomes more influential than interparticle stresses at depths greater than 1 m in sand and 100 m in clay. In clays, the variation of seismic velocity with water saturation is almost double the range predicted when only net overburden stress is considered to influence stress at the grain contacts. The proposed model calculates seismic velocities that compare well with measured field velocities from the literature.

Introduction

Current constitutive elastic models of granular materials are able to predict shallow (< 30 m) seismic velocities in sands (Bachrach *et al.*, 1998; Velea *et al.*, 2000), but can be improved to predict seismic velocities in clay-rich soils where additional interparticle stresses exist, caused by capillarity (Tinjum *et al.*, 1997) and cohesivity (Ikari and Kopf, 2011). Through improved elastic models, observed seismic velocity can be inverted (Eberhart-Phillips *et al.*, 1989; Aster *et al.*, 2012) to better estimate parameters such as water saturation, porosity, matrix elastic moduli, or pressure.

The influences of pore content, matrix composition, and pressure on elasticity can be related through the elastic wave equation by implementing fluid substitution theory (Gassmann, 1951) and granular contact theory (Mindlin and Deresiewicz, 1953).

Biot-Gassmann theory effectively explains the influence of pore constituent variations on elasticity and density of the porous media. When pore contents, such as water or air, have no shear resistance, the effective shear modulus is equal to the shear modulus of the granular matrix. In conventional Biot-Gassmann theory, elastic moduli of the granular matrix are considered constant. As water saturation increases in the pore space, a decrease in the seismic velocity is attributed to the Biot-Gassmann effect (Wulff and Burkhardt, 1997), because the bulk density increases more than the effective bulk modulus of the overall granular material.

Hertz-Mindlin contact theory is used to calculate the elastic moduli of elastic granular materials in terms of porosity, grain contact geometry, grain elasticity, and grain contact stress. Net overburden

stress (Eaton, 1969) is typically used in granular contact models to represent stress at the grain contacts and is the weight of the sediment above the grain contact minus the local pore pressure. Hertz-Mindlin theory predicts that seismic velocity (V) will increase as a power function of stress (σ) ($V \propto \sqrt[6]{\sigma}$) (Mindlin and Deresiewicz, 1953).

Total effective stress (Lu and Likos, 2006) (Appendix A) represents the average stress carried by the granular matrix and was first defined as total stress minus pore pressure (Terzaghi, 1943). Today the total effective stress equates to the sum of net overburden stress and interparticle stresses (Bishop, 1959; Lu and Likos, 2006); that will be the definition used for the remainder of this paper.

Interparticle stresses contribute to the total effective stress and include capillary stress arising from the interfacial tension between grains and the wetting phase (Tinjum *et al.*, 1997), negative pore water pressure (Rinaldi and Casagli, 1999), and physiochemical stresses caused by van der Waals attractions, electrical double layer repulsion, and chemical cementation effects (Ikari and Kopf, 2011). Interparticle stresses can be classified into stresses in fully saturated media (σ_{CO}), that confer cohesion to sediments, and stresses in unsaturated media that result as water saturation changes ($\sigma'_{S,}$ soil suction stress-Appendix A) (Lu and Likos, 2006). Interparticle stresses are important in the near-surface (0-100 m) because they increase the pressure at grain contacts and can be several orders of magnitude (MPa) larger than the net overburden stress. In the near-surface, interparticle stress influences on total effective stress have been examined in detail for engineering and agricultural purposes (Bishop, 1959; Lade and Boer, 1997), but have yet to be included in constitutive elastic models for predicting seismic velocity of granular material (Dvorkin *et al.*, 1999).

Net overburden stress estimation can be difficult at depths near a changing water table, because weight of sediment below the water table is effectively lowered by buoyancy (Turner, 1979). In this case, buoyancy is the displacement of water by sediments (Archimedes' Principle) and results in a decrease in total effective stress on the granular matrix and hence the seismic velocity.

Several field studies demonstrate that both net overburden stress and interparticle stresses, particularly in shallow unconsolidated sediments, are important to consider when developing constitutive elastic models. Vanapalli et al. (1997) measure a ~100 kPa increase (at 100 kPa of net overburden stress) in shear strength-- the resistance of a material to shear failure-- of a sandy-clay till, caused by changes in interparticle stresses as water saturation decreases. In shallow unconsolidated sediments, seismic velocities can be underestimated if interparticle stresses are excluded when calculating pressure at grain contacts. Lu and Sabatier (2009) document water saturation, temperature, stress, and compressional velocity in shallow soil over a two year period. The range in measured velocities (260-460 m/s) cannot be predicted by changes in net overburden stress (<5 kPa) and must also include changes in interparticle stresses (>350 kPa). In previous elastic models, the exclusion of interparticle stresses for the case of deep unconsolidated sediments remains valid where net overburden stresses are several orders of magnitude more than interparticle stresses (Dvorkin and Nur, 1996).

We propose a constitutive elastic model, suitable for use in unconsolidated clays as well as sands, and which estimates elastic moduli of elastic granular materials by extending conventional Hertz-Mindlin (Mindlin and Deresiewicz, 1953) and Biot-Gassmann (Gassmann, 1951) theory to incorporate interparticle stresses (Appendix A). Hertz-Mindlin and Biot-Gassmann theories are implemented to calculate effective bulk moduli and shear moduli for granular materials (mixture of grains, gas, and fluid) from bulk moduli and shear moduli of the individual grains. Seismic velocities are then calculated from these elastic moduli through the elastic wave equation (e.g., Ikelle and Amundsen, 2005) (Appendix A). An updated definition of total effective stress which includes interparticle stresses (Appendix A) is incorporated into Hertz-Mindlin theory. Because total effective stress changes with water saturation, the bulk modulus and the shear modulus of the granular matrix (K_{matrix} and G_{matrix}--

Appendix A) vary throughout the full range of saturations. The elastic moduli of the granular matrix increase as the net overburden stress increases with depth and vary with interparticle stresses as water saturations change. Traditionally, Biot-Gassmann theory estimates elastic properties of granular materials by varying the elastic properties of the pore space as the pore constituents change in concentration but assumes that the elastic properties of the granular matrix are constant. However, Biot-Gassmann theory can also account for changes in the elastic properties of the granular matrix during changes in water saturation by updating the reference elastic moduli of the matrix through Hertz-Mindlin theory (Appendix A).

The influence of interparticle stresses is demonstrated by calculating theoretical seismic velocities from physical properties of sand and clay (Table 1) with varied total effective stresses and water saturations. Results show that our modeled velocities are indistinguishable from those calculated from traditional Hertz-Mindlin and Biot-Gassmann methodologies at large confining pressures (>5 MPa) and low interparticle stresses (<2 kPa); however, calculated seismic velocities for materials with large interparticle stresses can be very different. As well, calculated seismic velocities successfully compared to measured field velocities (Lu and Sabatier, 2009) obtained at small confining pressures (<5 kPa) and over a large total effective stress range (>350 kPa) to validate the new model.

Table 1: Physical and theoretical properties and model parameters of sands and clays for seismic velocity calculations. Presented van Genuchten parameters (van Genuchten, 1980) are calibrated for capillary pressures in psi for sands and kPa in clays. Unrealistically low coordination numbers have been previously used to match slow seismic velocities in shallow sediments (Bachrach *et al.*, 1998; Velea *et al.*, 2000). The low coordination numbers (1) do not affect velocity trends.

Model Parameters	Sand	Reference	Clay	Reference
Grain Shear Modulus (Pa)	4.5×10^{10}	Mavko et al. (2003)	9.9×10^{9}	Mavko et al. (2003)
Grain Bulk Modulus (Pa)	3.66×10^{10}		2.5×10^{10}	
Grain Density (kg/m^3)	2650		2550	
Grain Poisson's Ratio	0.15		0.15	
Porosity	0.35		0.56	
Water Density (kg/m^3)	1000		1000	
Air Density (kg/m^3)	1.22		1.22	
Gravitational Acceleration (m/s^2)	9.81		9.81	
Coordination Number	1		1	
Van Genuchten n Fitting Parameter	5.69	Engel (2005)	2	Song et al. (2012)
Van Genuchten α Fitting Parameter (1/m)	4.56		0.01	
Irreducible Water Content	0.024		0.10	
Matrix Cohesion (Pa)	300	(Krantz, 1991)	16000	(Bishop, 1960)

Theoretical seismic velocity calculations

Besides the constants assumed in the model (Table 1), estimates of total effective stress and water saturation must be made in order to calculate seismic velocities. Total effective stress and water saturation changes drive velocity differences because they are the only variables that change within each case. Total effective stress for the theoretical models is calculated by adding net overburden stress from

the weight of the sediment column and interparticle stress from van Genuchten fitting parameters and water saturation (Song *et al.*, 2012) (Appendix A). For all cases, we calculate seismic velocities using either total effective stress or solely net overburden stress to highlight the influence of interparticle stresses. Theoretical seismic velocity is calculated over a range of water saturations at constant depth to show the significant contribution of interparticle stresses on seismic velocity in different soil types (Figure 1). We focus on using water saturation values greater than 10%, which is above residual water saturation, and less than 95% because compressional seismic velocities can increase over 10^3 m/s as water saturation approaches 100%. Normally, shallow soils are not fully saturated and observed velocities are in the order of 10^2 m/s. We also focus on this range of water saturations because interparticle stresses increase above a base value within this range. Above 95% water saturation soil suction stress becomes negligible.

Velocity-depth profiles (Figure 2A and B) are calculated for sands and clays with stationary water tables to illustrate the decreasing effect of interparticle stresses as depth and net overburden stress increase. In this case we estimate water saturation with depth from soil water characteristic curves (SWCC) (Appendix A). Pressure head-water saturation profiles converted from capillary pressure-water saturation curves (e.g. SWCC) (Figure 3) are consistent with natural water saturation profiles (Desbarats, 1995).

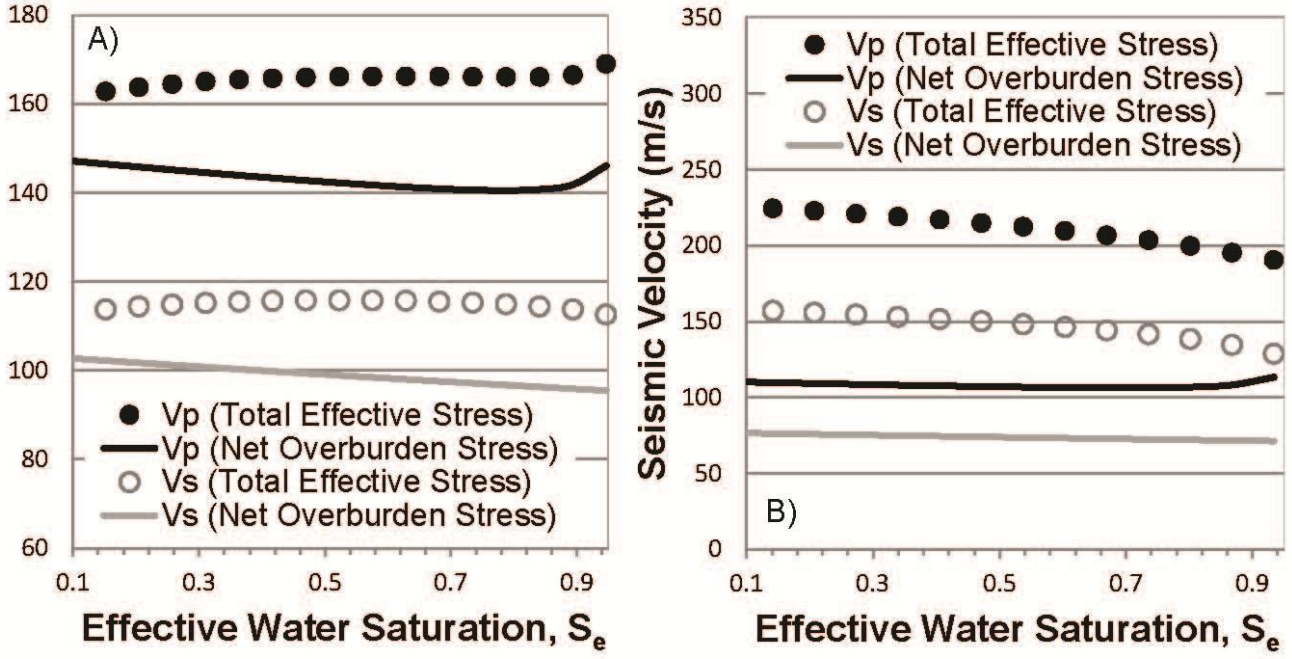

Figure 1: Compressional (V_P) and shear-wave (V_S) velocities are calculated for A) sand at 10 cm depth and B) clay at 1 m depth to emphasize the contribution of interparticle stresses.

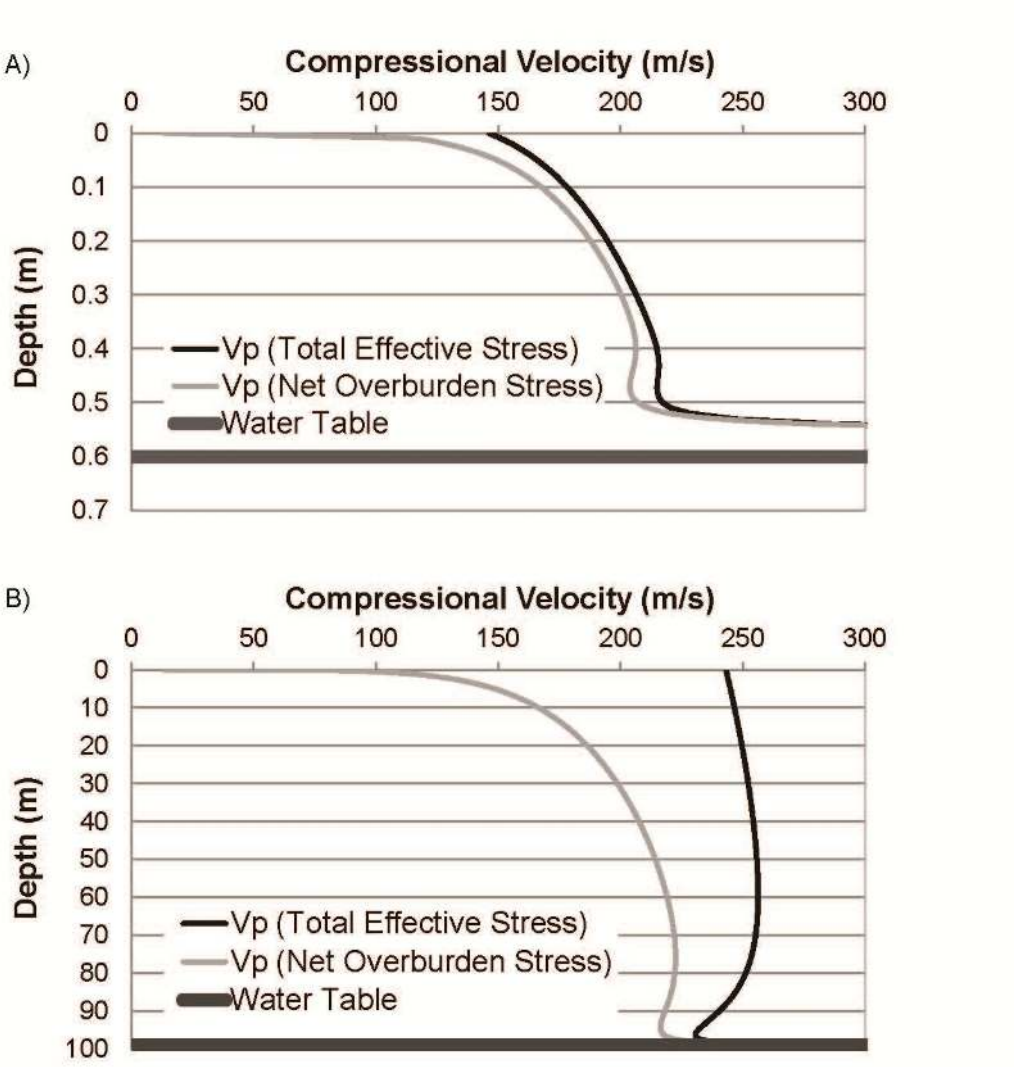

Figure 2: Seismic compressional wave velocities (V_P) calculated after pore fluid reaches steady-state equilibrium for A) sand and B) clay. Water table line (phreatic surface) shows where pressure head is equal to atmospheric pressure. Saturation at each depth is input into the model, calculated from soil parameters (Table 1).

Several additional assumptions are made in order to calculate the seismic velocities for comparison with measured field velocities. Calculations require reasonable estimations of water saturation and total effective stress, both of which are presented in literature (Lu and Sabatier, 2009). Total effective stress is input for the range of observed stresses. Total effective stress and water saturation measurements are highly variable so we simplify water saturation input by correlating several water saturation and total effective stress values from the raw data. Water saturation is highest (53%) at the lowest effective stress and is assumed to decrease linearly until it reaches its lowest value (10%) at the largest effective stress. This relationship appears to hold true (±2% S_w) for the presented measurements. Total effective stress correlates with water saturation because of soil suction stress. The increase in velocity caused solely by changes in bulk modulus and density of the pore space is compared to measured velocities to further illustrate that interparticle stresses must be included in velocity calculations.

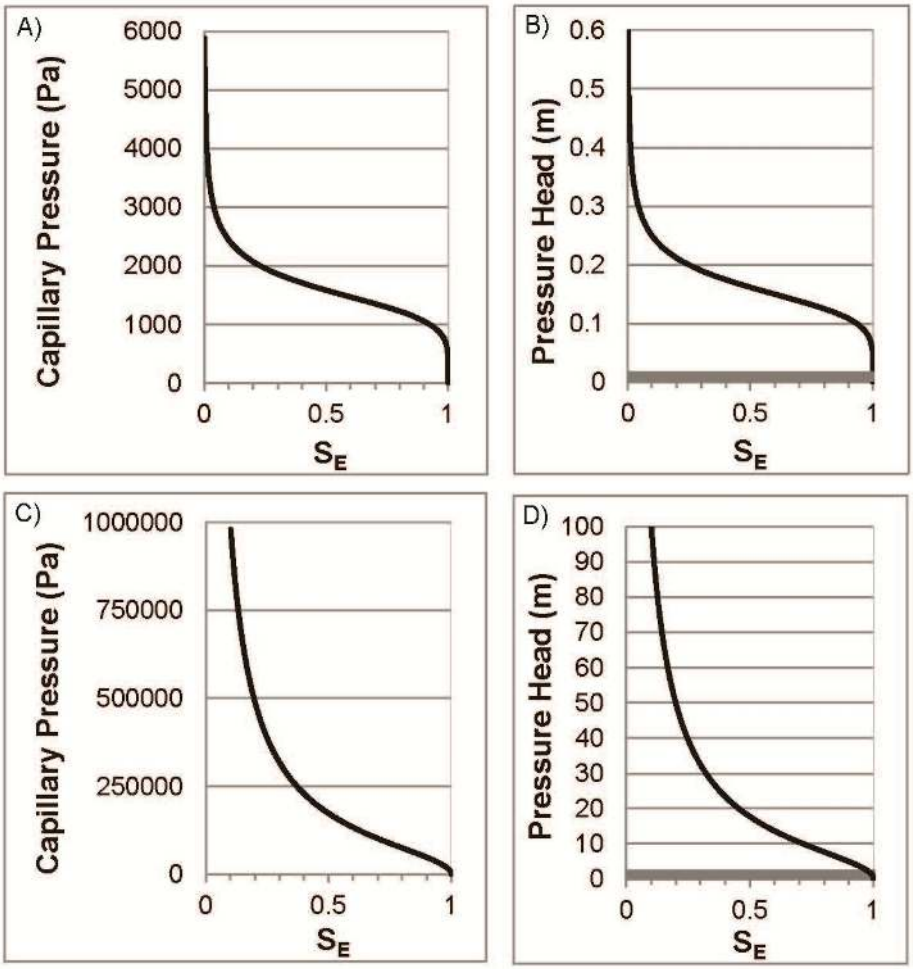

Figure 3: Soil-water characteristic curves for A) sand and C) clay calculated from van Genucthen fitting parameters (Table 1). The capillary pressures are converted to pressure head for input into velocity-depth models for B) sand and D) clay (Figure 3). The water tables are at 0 m pressure head.

Results

When interparticle stresses are included in constitutive elastic models, there is a significant difference in predicted seismic velocities from traditional models. When total effective stress is used to calculate pressure at the grain contacts instead of only net overburden stress, theoretical seismic velocities can be up to 20% larger in sands and up to 60% larger in clays. Over a range of 10-95% water saturation the predicted seismic velocity in sand increases with water saturation and the Biot-Gassmann effect is not apparent (Figure 1A). In clays, velocity decreases as water saturation increases (Figure 1B), but when interparticle stresses are considered the difference between the fastest and slowest velocities is twice as large. At shallow depths (0-100 m), clays and sands may have different seismic velocity trends with water saturation because of their respective interparticle stresses (Figure 4).

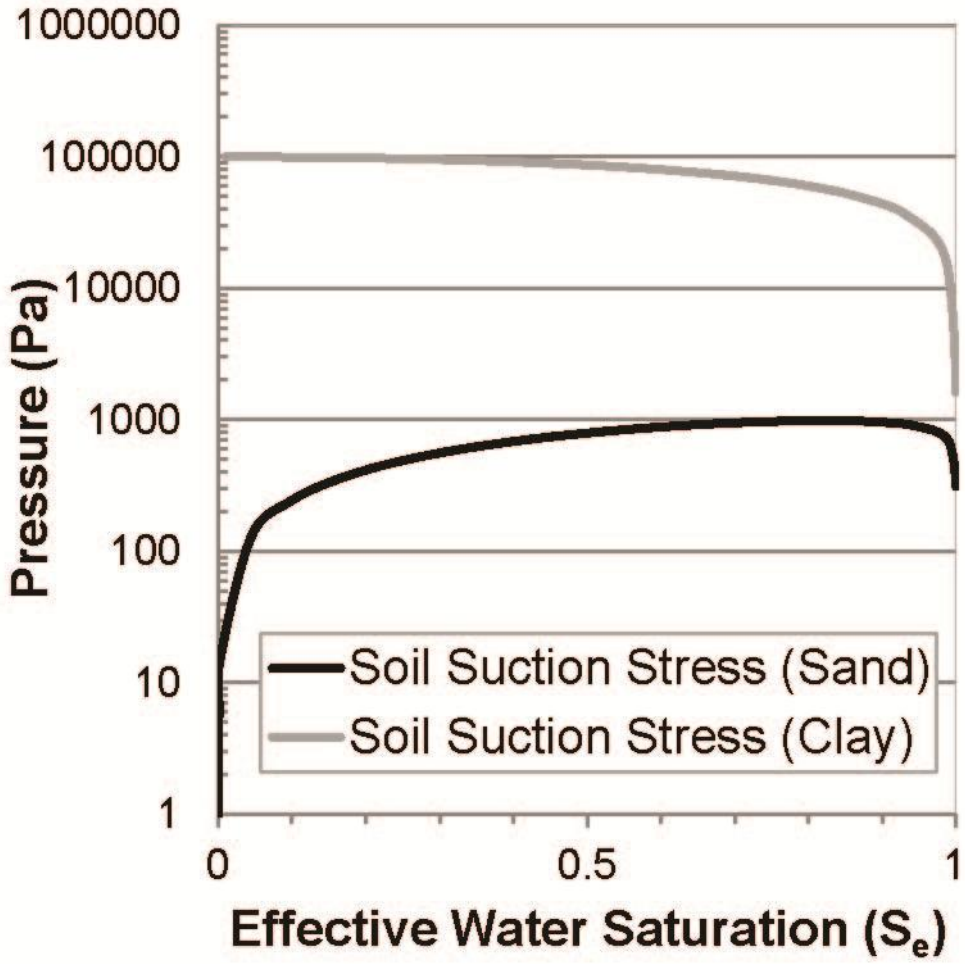

Figure 4: Calculated soil suction stress curves for sand and clay using the method by Song (2012).

Velocity-depth profiles calculated using either total effective stress or only net overburden stress are most different at the surface and converge near the water table (Figure 2A and 2B). Calculated velocities have similar trends as depth increases and net overburden stress becomes the largest component of total effective stress. For the modeled granular materials, net overburden stress equals the value of interparticle stresses at ~14 cm in sand and ~83 m in clay.

Theoretical velocities correlate well with field measured seismic velocities which increase as total effective stress increases and water saturation decreases (Lu and Sabatier, 2009) (Figure 5). Without interparticle stresses contributing to grain contact stress, we would expect pore constituent concentrations to be the main variables affecting seismic velocity. However, changes in the bulk modulus and density of the pore space only account for an ~14 m/s increase in seismic velocity. Large interparticle stresses (>20 kPa) are much more influential on shallow seismic velocities (<30 cm) than net overburden stress or pore constituent concentrations.

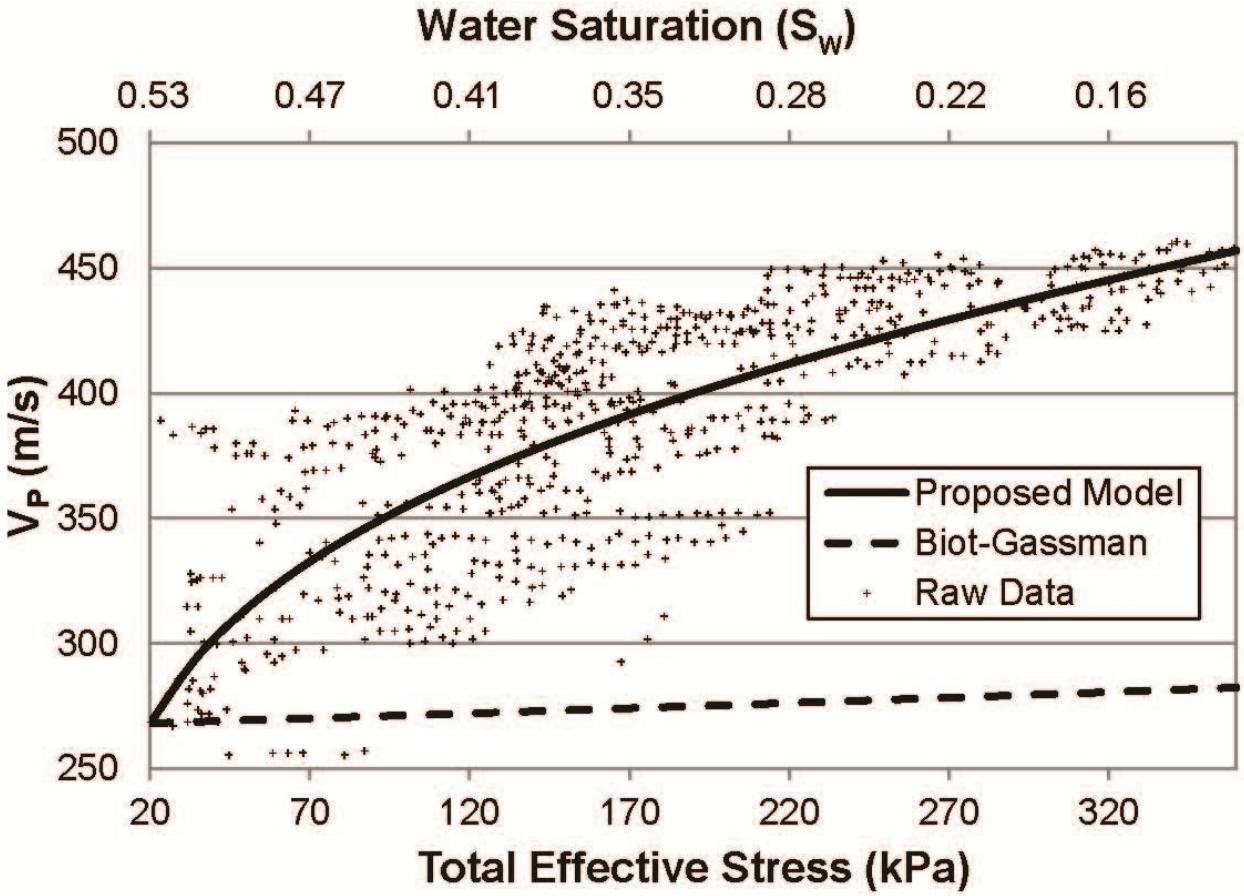

Figure 5: Model input parameters are for clay (Table 1) with the exception of coordination number, which is changed to 4.4 to provide the best fit to the data. Raw data are from Lu and Sabatier (2009).

Discussion

Interparticle stresses should be included in seismic velocity modeling of shallow unconsolidated sediments, even in sands which have very low capillary pressures and cohesion, but especially in clays which have very high interparticle forces. The large velocity variations measured by Lu and Sabatier (2009) at constant depths are better explained by interparticle stresses than density and elasticity changes during fluid substitution—these can only account for an ~8% velocity change (Figure 5). When predicting seismic velocities, interparticle stresses are particularly important at depths less than 1 m in sands and 100 m in clays. At these depths, net overburden stress becomes a larger component of total effective stress than interparticle stresses. The proposed model remains applicable at large depths (>1 km) where our calculated velocities at large net overburden stresses (>5 MPa) are indistinguishable from previous models (Dvorkin and Nur, 1996).

Total effective stress is a required parameter in the proposed model. In the absence of direct measurements, total effective stress can be estimated from the SWCC but specific temperature-pressure and wetting/drying conditions must be considered. Hysteresis in the SWCC for clays during wetting and drying cycles accounts for as much as 30% differences in capillary pressures and is attributed to a change in contact angle between the wetting phase and the solid surface (Pham *et al.*, 2005). Capillary pressure decreases by 3 kPa in sands as temperature increases from 20 to 80 °C (She and Sleep, 1998).

Some water table monitoring studies attribute longer seismic wave travel times to shallower water tables because of the Biot-Gassmann effect (Birkelo *et al.*, 1987; Bachrach *et al.*, 1998). In sands, calculations of seismic velocity that include interparticle stresses predict an increase in seismic velocity with increasing water saturation (Figure 2A) so that a lower seismic velocity may not be attributed solely to the Biot-Gassmann effect. Instead, the longer travel times can also be explained by a decrease in velocity caused by buoyancy. In normally-pressured sands, the net overburden stress gradient can decrease up to ~9800 Pa/m with the addition of water, due to buoyancy. Because of the decrease in the net overburden stress gradient, seismic velocities will decrease ($V \propto \sqrt{\sigma}$).

As water saturation decreases in clays, calculated velocities have twice the range predicted by effective bulk modulus and density changes of the pore space (Figure 1B). In comparison to sand, clay shows a larger variation in predicted velocities with changes in water saturation (Figure 1). This greater sensitivity of velocity to water saturation makes clays more suitable for water saturation modeling.

Conclusions

An improvement in our understanding of total effective stress (Lu and Likos, 2006) in constitutive elastic models allows improved predictions of seismic velocity in both shallow sands and clays. The added effect of interparticle stresses suppresses the Biot-Gassmann effect in shallow sediments. When interparticle stresses are included, as water saturation increases, the decrease in seismic velocity can be 100% larger than with prior models. A larger change in seismic velocity implies that water saturation can be modeled with more accuracy in shallow clays than in sands. At depths greater than 1 m in sands and 100 m in clays, net overburden stress becomes a larger component of total effective stress than interparticle stresses in the modeled granular materials. The proposed model predicts seismic velocities that fit well with field measured seismic velocities under low confining pressures (<5 kPa) and a large range of interparticle stresses (>350 kPa).

Acknowledgements

We would like to thank the following for their support with scholarships and a graduate assistantship to the first author: Southeast Louisiana Flood Protection Authority-East, American Petroleum Institute Delta Chapter of New Orleans, New Orleans Geological Society, Southeastern Geophysical Society, American Federation of Mineralogical Societies, Society of Exploration Geophysicists, Red River Desk and Derrick Club, Marathon Oil, Chevron Corporation, and especially to the LSU Department of Geology and Geophysics for their active support of graduate student research.

Appendix A

Formulae:

Elastic wave equation (e.g. Ikelle and Amundsen, 2005)

The influences of pore content, matrix composition, and pressure on elasticity are related through the elastic wave equation by implementing fluid substitution theory (Gassmann, 1951) and granular contact theory (Mindlin and Deresiewicz, 1953). The "*eff*" subscript is used to differentiate the elastic moduli of the bulk granular material from the elastic moduli of the granular matrix, pore space, or individual grains. Effective elastic moduli of the granular materials are calculated from Biot-Gassmann fluid substitution. Bulk density is calculated from the densities of the granular materials, the porosity, and the pore contents.

$$V_P = \sqrt{\frac{K_{eff}+\frac{4}{3}G_{eff}}{\rho_{Bulk}}} \qquad V_S = \sqrt{\frac{G_{eff}}{\rho_{Bulk}}}$$

where V_P is the P-wave velocity, V_S is the S-wave velocity, K_{eff} is the effective bulk modulus, G_{eff} is the effective shear modulus, and ρ_{Bulk} is the bulk density.

Biot-Gassmann fluid substitution (Gassmann, 1951; Biot, 1956)

Biot-Gassmann theory effectively explains the influence of pore constituent variations on elasticity and density of the porous media. When pore contents such as water or air have no shear resistance, the effective shear modulus is equal to the shear modulus of the granular matrix.

$$\frac{K_{eff}}{K_0-K_{eff}} = \frac{K_{matrix}}{K_0-K_{matrix}} + \frac{K_{pore}}{\phi(K_0-K_{pore})} \quad G_{eff} = G_{matrix}$$

where K_0 is the bulk modulus of the grains and K_{pore} is the bulk modulus of the pore space. The bulk modulus of the pore space is a weighted harmonic mean of the bulk moduli of the pore constituents (Gassmann, 1951). When the two pore constituents are water and air, the bulk modulus of the pore space (K_{pore}) can be calculated:

$$\frac{1}{K_{pore}} = \frac{S_w}{K_{water}} + \frac{1-S_w}{K_{air}}$$

where S_w is water saturation, K_{water} is the bulk modulus of water, and K_{air} is the bulk modulus of air. In conventional Biot-Gassman, elastic moduli of the granular matrix are considered to be constant. Note that variables with a "matrix" subscript are used instead of the "dry" subscript used in conventional Biot-Gassmann fluid substitution equations (Bachrach et al., 1998). The new notation is used to better show that we are using a reference matrix elasticity, whether wet or dry. In unconsolidated sediments G_{eff} is equal to G_{Matrix} at a particular depth and water saturation, but neither is constant throughout the full range of saturations. The depth and water saturation dependence of matrix elasticity is due to total effective stress contributions of net overburden stress and soil suction stress, respectively. Matrix elasticity is calculated using Hertz-Mindlin theory.

Hertz-Mindlin granular contact theory (Mindlin and Deresiewicz, 1953)

Because we are estimating the elasticity of unconsolidated granular materials, matrix elastic moduli are calculated using Hertz-Mindlin theory which calculates the elastic moduli of a random packing of spheres in terms of grain contact geometry, grain elasticity, and total effective stress.

$$K_{Matrix} = \sqrt[3]{\frac{n^2(1-\Phi)^2G^2}{18\pi^2(1-\nu)^2}P}$$

$$G_{Matrix} = \frac{5-4\nu}{5(2-\nu)}\sqrt[3]{\frac{3n^2(1-\Phi)^2G^2}{2\pi^2(1-\nu)^2}P}$$

where n is grain coordination number, G is the grain shear modulus, ν is the grain poisson's ratio, K_{Matrix} is the bulk modulus of the skeletal matrix, G_{Matrix} is the shear modulus of the skeletal matrix, and P is the total effective stress.

Total effective stress (Lu and Likos, 2006)

Total effective stress at the grain contacts is used to calculate matrix elasticity in Hertz-Mindlin theory. In the absence of direct measurements, total effective stress can be estimated from the sum of forces acting on the granular matrix:

$$P = (\sigma_T - u_a) + \sigma'_S + \sigma_{CO}$$

where σ_T is the total external stress, u_a is pore-pressure, σ'_S is soil suction stress (Lu and Likos, 2006), and σ_{CO} is apparent tensile stress at the saturated state caused by cohesive or physiochemical forces (Bishop *et al.*, 1960). Physiochemical forces are local forces arising from individual contributions from van der Waals attractions, electrical double layer repulsion, and chemical cementation effects (Lu and Likos, 2006). Saturated cohesion (σ_{CO}) is constant for different soil types and taken from literature (Table 1). Other total effective stress components are accounted for in separate sections of the appendix.

Net overburden stress (Terzaghi et al., 1996)

If normal stress from the weight of the sediment is much larger than horizontal stresses, the difference $(\sigma_T - u_a)$ becomes net overburden stress and can be calculated using the following formula,

$$Net\ overburden\ stress = \sigma_T - u_a = \rho_{Bulk} g h_1 + (\rho_{Bulk} - \rho_{Water}) g h_2$$

where ρ_{Matrix} is the density of the solid matrix, ρ_{Water} is the density of water, g is gravitational acceleration, h_1 is the height of the sediment column not influenced by buoyancy, and h_2 is the height of the sediment column supported by buoyancy. Under normal pore pressure conditions, pore-pressure is calculated:

$$u_a = \rho_{water} g h_2$$

SWCC fitting equation (van Genuchten, 1980)

The work of van Genuchten (1980) is used to empirically fit capillary pressures and water saturations for different sediments because fitting parameters (α and n) can be used to calculate soil suction stress.

$$S_E = \frac{\theta - \theta_r}{\theta_s - \theta_r} = \left[\frac{1}{1 + [\alpha(u_a - u_w)]^n}\right]^{\frac{n-1}{n}}$$

where S_E is effective saturation, θ is the volumetric water content, θ_r is the residual water content, θ_s is the saturated water content which is equivalent to porosity, α and n are van Genuchten (1980) empirical fitting parameters, and $(u_a - u_w)$ is capillary pressure. A SWCC is useful if water saturations need to be estimated above a given water table. A SWCC can be converted into a pressure head-water saturation profile by solving the above equation for capillary pressure ($u_a - u_w$), and setting it equal to the weight of the water column supported above the water table (pore pressure equation). The pressure head (height above the water table) can then plotted against water saturation, creating a pressure head-water saturation profile (Figure 4).

Soil suction stress curve (Song *et al.*, 2012)

Van Genuchten fitting parameters, obtained from fitting a SWCC, are used to calculate soil suction stress.

$$\sigma'_s = -\frac{S_E}{\alpha}\left(S_E^{\frac{n}{1-n}} - 1\right)^{\frac{1}{n}}$$

Bulk density (Bourbie *et al.*, 1992)

Bulk density is the weighted mean of matrix and pore space densities. When the pore space is filled by a combination of water and air the equation for bulk density becomes.

$$\rho_{Bulk} = \phi(S_w \rho_{water} + (1 - S_w)\rho_{air}) + (1 - \phi)\rho_{grain}$$

where ϕ is the porosity of the skeletal matrix, S_W is the water saturation, ρ_{water} is the density of water, ρ_{air} is the density of air, and ρ_{grain} is the grain density. Bulk density is needed for input into the elastic wave equation.

References

Aster, R.C., Borchers, B., Thurber, C.H., 2012. Parameter estimation and inverse problems. Academic Press.

Bachrach, R., Dvorkin, J., Nur, A., 1998. High-resolution shallow-seismic experiments in sand. Part 2: Velocities in shallow unconsolidated sand. Geophysics 63, 1234-1240.

Biot, M.A., 1956. Theory of elastic waves in a fluid-saturated porous solid. 1. Low frequency range. Journal of the Acoustic Society of America 28, 168-178.

Birkelo, B.A., Steeples, D.W., Miller, R.D., Sophocleous, M., 1987. Seismic Reflection Study of a Shallow Aquifer During a Pumping Test. Ground Water 25, 703-709.

Bishop, A.W., 1959. The principle of effective stress. Tek. Ukeblad 106, 859-863.

Bishop, A.W., Alpan, I., Blight, G., Donald, I., 1960. Factors controlling the strength of partly saturated cohesive soils.

Bourbie, T., Coussy, O., Zinszner, B., Junger, M.C., 1992. Acoustics of Porous Media. Acoustical Society of America Journal 91, 3080.

Desbarats, A., 1995. Upscaling capillary pressure-saturation curves in heterogeneous porous media. Water Resources Research 31, 281-288.

Digby, P.J., 1981. The Effective Elastic Moduli of Porous Granular Rocks. Journal of Applied Mechanics 48, 803-808.

Dvorkin, J., Nur, A., 1996. Elasticity of high-porosity sandstones: Theory for two North Sea data sets. Geophysics 61, 1363-1370.

Dvorkin, J., Prasad, M., Sakai, A., Lavoie, D., 1999. Elasticity of marine sediments: Rock physics modeling. Geophysical Research Letters 26, 1781-1784.

Eaton, B., 1969. Fracture gradient prediction and its application in oilfield operations. Journal of petroleum technology 21, 1353-1360.

Eberhart-Phillips, D., Han, D., Zoback, M., 1989. Empirical relationships among seismic velocity, effective pressure, porosity, and clay content in sandstone. Geophysics 54, 82-89.

Engel, J., Schanz, T., Lauer, C., 2005. State parameters for unsaturated soils, basic empirical concepts. In: Schanz, T. (Ed.), Unsaturated Soils: Numerical and Theoretical Approaches. Springer Berlin Heidelberg, pp. 125-138.

Gassmann, F., 1951. Uber die Elastizitat poroser Medien. Veirteljahrsschrift der Naturforshenden Gesellshaft in Zurich 96, 1-23.

Ikari, M.J., Kopf, A.J., 2011. Cohesive strength of clay-rich sediment. Geophysical Research Letters 38, L16309.

Ikelle, L., Amundsen, L., 2005. Introduction to petroleum seismology. Society of Exploration Geophysicists, Tulsa, Okla.

Krantz, R.W., 1991. Measurements of friction coefficients and cohesion for faulting and fault reactivation in laboratory models using sand and sand mixtures. Tectonophysics 188, 203-207.

Lade, P.V., Boer, R.D., 1997. The concept of effective stress for soil, concrete and rock. Géotechnique. 47, 61.

Lu, N., Likos, W.J., 2006. Suction Stress Characteristic Curve for Unsaturated Soil. Journal of Geotechnical and Geoenvironmental Engineering. 132, 131.

Lu, Z., Sabatier, J.M., 2009. Effects of soil water potential and moisture content on sound speed. Soil Science Society of America Journal 73, 1614-1625.

Mavko, G., Mukerji, T., Dvorkin, J., 2003. The Rock Physics Handbook: Tools for Seismic Analysis of Porous Media. Cambridge University Press.

Mindlin, R.D., Deresiewicz, H., 1953. Elastic Spheres in Contact Under Varying Oblique Forces. Journal of Applied Mechanics 20, 327.

Pham, H., Fredlund, D., Barbour, S., 2005. A study of hysteresis models for soil-water characteristic curves. Canadian Geotechnical Journal 42, 1548-1568.

Rinaldi, M., Casagli, N., 1999. Stability of streambanks formed in partially saturated soils and effects of negative pore water pressures: the Sieve River (Italy). Geomorphology 26, 253-277.

She, H.Y., Sleep, B.E., 1998. The effect of temperature on capillary pressure-saturation relationships for air-water and perchloroethylene-water systems. Water Resources Research 34, 2587-2597.

Song, Y.-S., Hwang, W.-K., Jung, S.-J., Kim, T.-H., 2012. A comparative study of suction stress between sand and silt under unsaturated conditions. Engineering Geology 124, 90-97.

Terzaghi, K., 1943. Theoretical soil mechanics. Wiley, New York.

Terzaghi, K., Peck, R.B., Mesri, G., 1996. Soil mechanics in engineering practice. Wiley-Interscience.

Tinjum, J.M., Benson, C.H., Blotz, L.R., 1997. Soil-Water Characteristic Curves for Compacted Clays. Journal of Geotechnical and Geoenvironmental Engineering 123, 1060-1069.

Turner, J.S., 1979. Buoyancy effects in fluids. Cambridge University Press.

van Genuchten, M.T., 1980. A Closed-form Equation for Predicting the Hydraulic Conductivity of Unsaturated Soils. Soil Science Society of America Journal 44, 892-898.

Vanapalli, S., Fredlund, D., Pufahl, D., 1997. Comparison of saturated-unsaturated shear strength and hydraulic conductivity behavior of a compacted sandy-clay till. Proceedings of the 50 th Canadian Geotechnical Conference, pp. 625-632.

Velea, D., Shields, F.D., Sabatier, J.M., 2000. Elastic Wave Velocities in Partially Saturated Ottawa Sand.

Wulff, A.M., Burkhardt, H., 1997. Dependence of seismic wave attenuations and velocities in rock on pore fluid properties. Physics and Chemistry of the Earth 22, 69-73.